A full Stokes imaging polarimeter based on a consumer CMOS camera

Sara Peña-Gutiérrez, María Ballesta, Santiago Royo

Sara Peña-Gutiérrez, María Ballesta, Santiago Royo, "A full Stokes imaging polarimeter based on a consumer CMOS camera," Proc. SPIE 11059, Multimodal Sensing: Technologies and Applications, 1105913 (21 June 2019); doi: 10.1117/12.2525706

SPIE.

Event: SPIE Optical Metrology, 2019, Munich, Germany

A full Stokes imaging polarimeter based on a consumer CMOS camera

Sara Peña-Gutiérrez[a], Maria Ballesta[a], and Santiago Royo[a]

[a]Centre de Desenvolupament de Sensors, Instrumentació i Sistemes (CD6), Universitat Politècnica de Catalunya, Rambla Sant Nebridi 10, E08222, Terrassa, Spain

ABSTRACT

Nowadays, taking advantage of polarization allows enhancing the contrast of a detected object and extending the information of the scene compared to conventional intensity imagery, as the information added by polarimetric images is complementary to intensity ones. Using polarization has a wide interest in space exploration, earth remote sensing, machine vision and biomedical diagnosis, and is extending its use to several applications. Here, we present a basic imaging polarimeter which measures the full Stokes vector of the scene based on a division of time structure, based on a consumer CMOS camera. The polarization state of partially or fully polarized light can be represented by means of the Stokes vector, which is the goal of the measurement. However, due to its nature, the components of the Stokes vector cannot be measured directly, as they must be recovered from a set of intensity measurements. In the paper the results show the measured intensity at 632nm and the recovered Stokes data produced by the determined data reduction matrix at six reference polarization states, as well as the theoretical and recovered Stokes parameters from the calibration experiment. The root mean square (RMS) errors are below 10% . Therefore, this system can provide a well-conditioned data reduction matrix for noise immunity and the spectral range can be widened by using white light and a monochrome camera.

Keywords: Imaging polarimetry, polarization, machine vision

1. INTRODUCTION

Polarimetry has emerged over the past four decades as a powerful tool for image classification. It provides a completely different source of information largely uncorrelated with spectral and intensity images. Applications in imaging polarimetry have been found in remote sensing,[1,2] sensing through diffusive media like fog or smoke,[3–5] aerosol characterisation,[6] non-invasive cancer diagnostics[7,8] or astrophysics,[9] among others.

Imaging polarimetry consists of the measurement of the polarization state of light across the scene to take advantage of its features in order to obtain additional information. Such information is usually obtained as a local Stokes vector distribution. Unfortunately, such a vector cannot be directly measurable with a single measurement, as in the case of intensity. Theoretical parameters and procedures have been developed in order to calculate the Stokes vector with a minimum of four independent intensity measurements. Changes of polarization in a scene can give information on surface features like shape, shading and roughness. This information is, as mentioned, uncorrelated with the information recovered by conventional intensity or spectral measurements, becoming a field of interest in machine vision applications, to e.g. detect objects or segment them inside a complex image.

In this paper a time division imaging polarimeter based on a consumer CMOS camera is described in detail. This device is calibrated by extending the improved method developed for conventional polarimeters to imaging polarimeters. This method has the advantage to perform properly without the need to fully characterizing the Mueller matrix of the system, as would be needed using the Fourier modulation technique. The proposed method allows to calibrate the system using reference polarization states (RPS) regardless the media under analysis, and

Further author information: (Send correspondence to S.P.G.)
S.P.G.: E-mail: sara.pena.gutierrez@upc.edu, Telephone: +34 93 7398905
M.B.: E-mail: maria.ballesta@upc.edu, Telephone: +34 93 7398905
S.R.: E-mail: santiago.royo@upc.edu, Telephone: +34 93 7398904

Multimodal Sensing: Technologies and Applications, edited by Ettore Stella, Shahriar Negahdaripour, Dariusz Ceglarek, Christian Möller, Proc. of SPIE Vol. 11059 1105913 · © 2019 SPIE · CCC code: 0277-786X/19/$21 · doi: 10.1117/12.2525706

is different from the usual method defined to directly obtain the Stokes parameters, and thus, allows to introduce RPS that may improve the recovery of the parameters reducing the errors and the presence of noise.

The paper has been organized as follows: the polarization basis and the measurement technique are explained in Section 2 to provide the theoretical framework. Then, the methodology is described in Section 3, followed by the presentation of the results in Section 4. Finally, the general conclusions are presented in Section 5.

2. DESCRIPTION OF THE MEASUREMENT TECHNIQUE

Obtaining the state of polarization of light is not straightforward. Due to its vectorial nature, it is needed to measure a number of different parameters, which are known as the Stokes parameters. These parameters were developed to express the state of light by means of 4 normalised scalar numbers, which are directly measurable:

$$\vec{S} = \begin{pmatrix} S_0 \\ S_1 \\ S_2 \\ S_3 \end{pmatrix} = \begin{pmatrix} |E_x|^2 + |E_y|^2 \\ |E_x|^2 - |E_y|^2 \\ 2Re(E_x E_y^*) \\ 2Im(E_x E_y^*) \end{pmatrix} \tag{1}$$

where S_0, S_1, S_2, and S_3 describe, respectively, the total intensity of light, the prevalence of the linear polarization state at 0^o over 90^o, the prevalence of the linear polarization state at 45^o over 135^o, and the prevalence of the right circular state over the left circular state, respectively. These parameters take values between -1 and 1 depending on the field component prevalence.

In order to get these parameters, it is necessary to perform a minimum of 4 independent intensity measurements at different polarization states to solve the linear system:

$$\vec{S} = \mathbf{W} \cdot \vec{I} \tag{2}$$

where $\vec{S}$ is the Stokes vector, $\mathbf{W}$ is the so-called measurement matrix of the system and $\vec{I}$ is the intensity vector containing the N measurements at the different polarization states.

Hence, the polarimetric image is obtained by solving Eq.(2) pixel by pixel, returning the complete Stokes vector at each pixel. However, the system must be calibrated before performing polarization imaging experiments in order to determine the measurement matrix $\mathbf{W}$, which will give the final Stokes vector.

Such a calibration procedure is performed using the data reduction matrix technique (DRM), where no *a priori* knowledge of the Mueller matrix of the system is required, thus making it applicable in multiple environments. This method allows determining $\mathbf{W}$ by means of singular value decomposition (SVD), by performing N intensity measurements corresponding to N different configurations of the polarization elements of the polarization state analyzer (PSA). Moreover, M different RPS are generated , for which their Stokes vectors are theoretically known $\vec{S_i}$ (i=0,1,...,M). Thus, the Eq.(2) can be rewritten as a linear matrix equation:

$$\mathbf{S} = \mathbf{W} \cdot \mathbf{I} \tag{3}$$

It usually happens in practice that when calculating the pseudoinverse of the matrix $I \cdot I^T$ is not mathematically well-conditioned. The situation leads to large variations in the calculated $\mathbf{W}$. A solution to this issue[10] is to use SVD in order to recover the pseudoinverse of $\mathbf{I}$. Since the Stokes vector has four degrees of freedom, the range of $\mathbf{I}$ should have four dimensions. Therefore, it should only have four single values. It is often recommended[10] to use the truncated pseudoinverse, setting to zero all that single values that are smaller than the four major single values, to compensate experimentl errors.

Once the system is calibrated, a map of the four Stokes vectors can be recovered at each pixel of the image, solving Eq.(2) pixel by pixel, as well as some maps of advanced parameters related to polarization such as the degree of polarization (DOP), degree of linear polarization (DOLP) and degree of circular polarization (DOCP), which can be calculated from the Stokes parameters by means of the following expressions:

$$DOP = \frac{\sqrt{S_1^2 + S_2^2 + S_3^2}}{S_0} \quad (4) \qquad DOLP = \frac{\sqrt{S_1^2 + S_2^2}}{S_0} \quad (5) \qquad DOCP = \frac{S_3}{S_0} \quad (6)$$

3. EXPERIMENTAL PROCEDURE

In this section, the experimental procedure of obtaining polarimetric images using a simple division of time polarimeter is described in detail. In order to achieve the final images, first the calibration experiment needs to be designed and executed. Once a good calibration matrix of the imaging system is determined, the acquisition of the final polarimetric images is carried out. Thus, we will have two independent set-ups, one for calibration and another one for real-world imaging.

3.1 Calibration set-up

The initial design is differentiated in two main parts: the illumination optics and the imaging optics (see Fig. 1). The illumination optics consists in a pig-tailed laser of wavelength 632nm attached to an integrating sphere in order to erase any signal of polarization and to spatially uniformize the beam. Next, a Polarization States Generator (PSG) composed by a linear polarizer and two circular polarizers mounted on a manual rotator will generate the RPS for calibration. Afterwards, an achromatic lens of large focal length f_1 (100mm) is set to control the beam size and minimize errors in the illumination. The imaging optics consists in a PSA, which allows to measure the desired polarization state, followed by a telescope integrated in the set-up to enlarge the beam size to cover almost completely the active area of the sensor, which is a Canon EOS1000 commercial camera with a CMOS RGB sensor. The PSA is compound by a quarter wave-plate (QWP) and a linear polarizer mounted on a manual rotator to select the preferred polarization configuration. The schematics of the setup and the actual setup mounted are presented in Fig.1 .

Taking advantage of the set-up explained before, two types of calibrations must be addressed. The first one is the radiometric calibration. It consists in removing the background effect caused by the components and the detector offset. A spatially uniform unpolarised source can be used for this calibration. Afterwards, the aim of the polarization calibration is to determine the actual data reduction matrix **W** of the system. This second calibration is based on the improved DRM method, previously explained in Sec. 2, which has the advantage of considering the higher order effects such as multiple reflections between or within the optical devices (very common in this type of set-ups), imperfect analysers and QWPs, and residual birefringence. The reconstruction accuracy of the Stokes parameters is only limited by the uncertainties and inaccuracies in the RPS.

The calibration procedure consists in producing several RPS, which are measured by the PSA at the optimum angles chosen for recovery. The polarization states selected to comprise the set of measurements for calibration are six: four linear polarization states at angles $0^o, 45^o, 90^o, 135^o$ and two circular states: right (RC) and left circular (LC). To produce the various linear RPS, a standard linear polarizer is rotated manually from 0^o to 180^o in steps of 10^o. To produce circularly polarized light, the linear polarizer was replaced by standard LC and RC polarizers. A total of 114 images for the 21 RPS were recorded in the polarimetric calibration experiment.

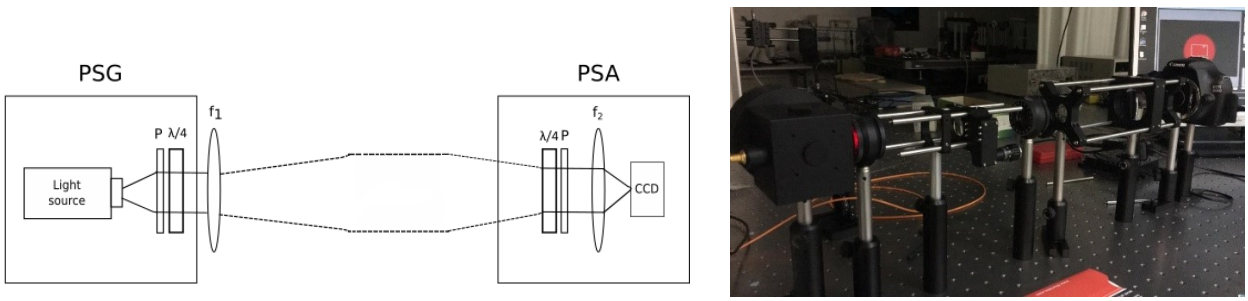

Figure 1. Scheme of the calibration set-up (top). DoT imaging polarimeter set-up already mounted in the optical bench (bottom).

3.2 Polarimetric imaging set-up

After determining the measurement matrix through calibration, the polarimetric images are ready to be taken. As starting images, some polarimetric images in transmission were acquired using the same six states of the PSA, as we did in the calibration procedure described. After acquiring the six images, at each pixel the different Stokes vector maps were calculated by solving Eq.(2). Afterwards, following the same procedure, a second experiment was performed measuring polarization from the reflected light of a plastic box with a linear sheet polarizer placed at an oblique angle illuminated with spatial uniform light from the integrating sphere, in order to detect local changes in materials or polarization behavior.

4. RESULTS

The results of the experiments described in the previous section are presented in the following. One key aspect to evaluate is the accuracy of the calibration performed, which needs to be validated before starting image acquisition. Once it is evaluated and considered to be sufficient, several imaging experiments are performed to see the response of the set-up when acquiring polarimetric images.

4.1 Calibration results

Once the calibration is performed, the data obtained must be processed to evaluate the accuracy of the determined **W** matrix. Fig.2 shows the average value of the measured intensity corresponding to the different RPS and the recovered data produced by the determined **W**. The evolution of the intensities in the linear RPS is fully consistent with the Malus law. It may be noticed how the recovered intensity using the calculated **W** matrix fits very well to the measured data, yet the intensities in the circular polarization modulation channels (plotted as linear states 190 and 200 of the PSG) deviate from the mean value of the sum of I_0 and I_{90}. This is mainly due to the deviation of the retardance and the azimuth of the achromatic QWP composing the PSA. Since the **W** matrix is measured directly, the retardance error will be included in the recovered Stokes vectors.

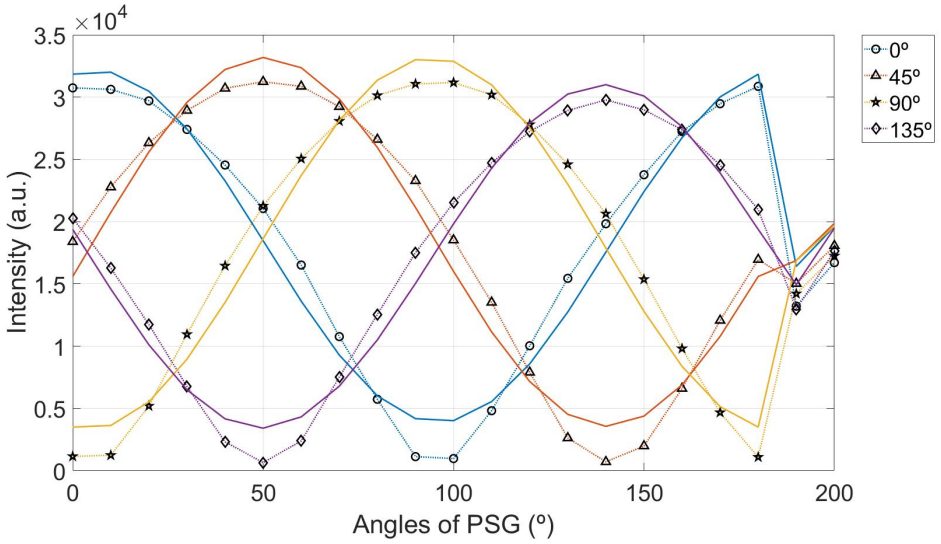

Figure 2. Mean value of the intensity at the different states of the measurement calibration set. The dashed lines with symbols represent the measured data at the different RPS. The solid lines represent the recovered intensity from calculated **W** matrix.

We choose the DOP as the figure of merit to depict the accuracy of the determined **W** matrix. Fig.3 (left) shows the DOP for all the RPS, applying Equations 4-6. Points correspond to the values of DOP, and the continuous lines to those of DOLP and DOCP. For the linear RPS, the theoretical values of the DOP and DOLP must be maximum (1.0, normalized) and minimum (0.0) for DOCP, meanwhile for the circular states the values of DOP and DOCP are 1.0 and for the DOLP is 0. The deviation between the recovered and the theoretical DOP,

DOLP and DOCP is presented in Fig.3 (right). The maximum deviations are lower than 10% in all cases. As main conclusion, the data reconstruction matrix determined from the mean value of the sensor area and the 21 RPS can be used for the reconstruction of full-Stokes parameters with an uncertainty level below 10%, within reasonable experimental error.

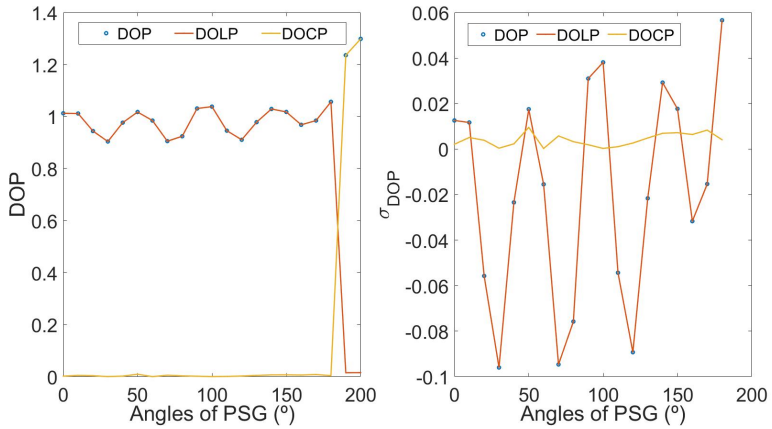

Figure 3. DOP at each RPS (left). Deviation of the recovered from the theoretical DOP at each RPS. Angles 190^o and 200^o correspond to RC and LC states, respectively, in order to preserve the same graphical representation (right).

Using the average measured intensity for each RPS and the determined **W** matrix, their related Stokes vectors may be recovered. Fig.4 (left) shows the resulting Stokes parameters based on the improved method of DRM[10] for calibration and their errors. The recovered data (solid line) shows small deviations from the theory (asterisks) that could not be described by the simplified description of the polarimeter, although the recovered data fits very well the expected values, specially in the linear states. Fig.4 (right) plots the RMS deviation of all the values of the Stokes parameters recovered. The RMS errors obtained are below 10% in the linear polarization states and around 20% just for the first Stokes value in the circular polarization. The difference in the circular states is attributed to imperfections in the circular polarizer and the QWP. Their detailed characterization is part of our future work.

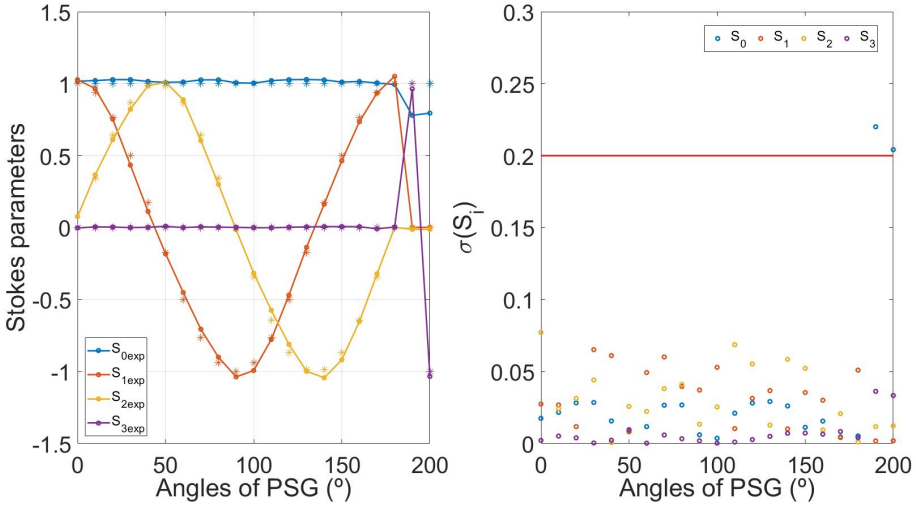

Figure 4. On the left, recovered (solid line) and theoretical (asterisks) Stokes parameters obtained using the PSG. On the right, RMS error between the recovered and the theoretical parameters. Angles 190^o and 200^o correspond to the RC and LC states.

4.2 Polarimetric images

The next step is to use the characterized matrix in order to capture polarimetric images and test the usability of the system. To do so, two different applications were approached. In the first experiment, we show the polarimetric images obtained through a linear polarizer at 45^o. In Fig. 5, we can appreciate the maps related to the recovered Stokes parameters, recovered pixel by pixel. Grayscale levels code the value of the parameter at each pixel, being black close to zero and white close to 1. As expected, the third parameter S_2 is significantly larger than S_1 and S_3 since it indicates the presence of linear polarization at 45^o. This is supported by computing the DOP, DOLP and DOCP values at each pixel generating the three maps shown below in Fig. 6 where maximum values of DOP and DOLP and a minimum value of DOCP indicate the presence of light with linear polarization. Thus, the measured results are consistent with the polarization states expected.

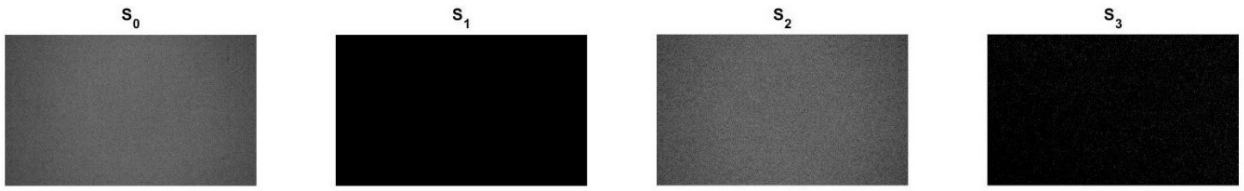

Figure 5. Maps of the four Stokes parameters for an image in transmission of a linear state at 45^o.

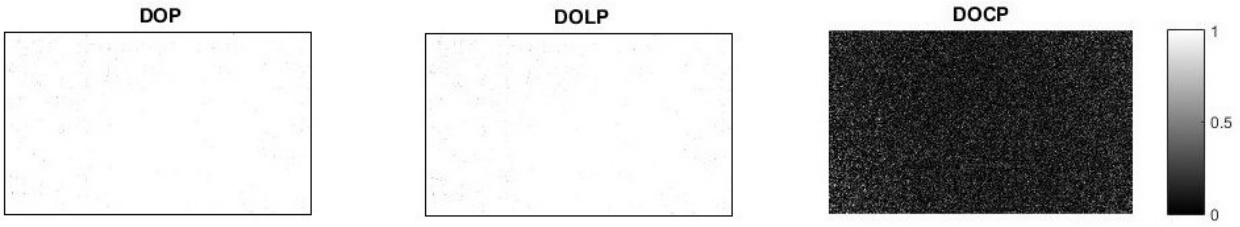

Figure 6. Maps of the recovered DOP, DOLP and DOCP for an image in transmission of a linear state at 45^o.

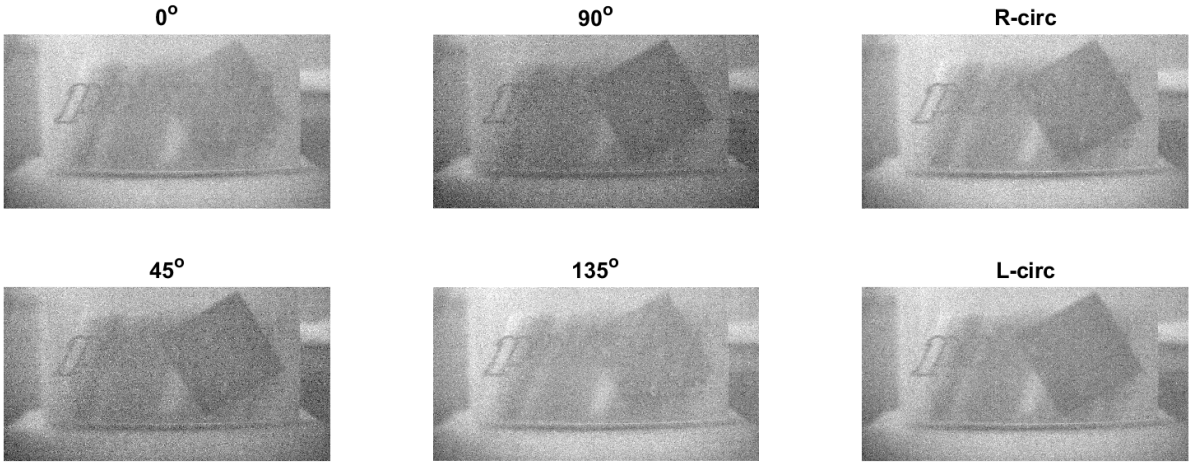

Figure 7. Maps of the intensity values in the six calibration channels from the reflection of the scene containing a linear polarizer at a random angle.

In the second experiment, going a step further, we measured the polarization of a controlled scene using the reflected light, using ambient illumination. A linear sheet polarizer located at an oblique azimuth angle is imaged through the system, as seen in Fig.7. The DOP maps can be appreciated in Fig. 8, and it is remarkable the presence of a whitest area in the DOP and DLP plots, corresponding to the position of the oblique polarizer within the scene.

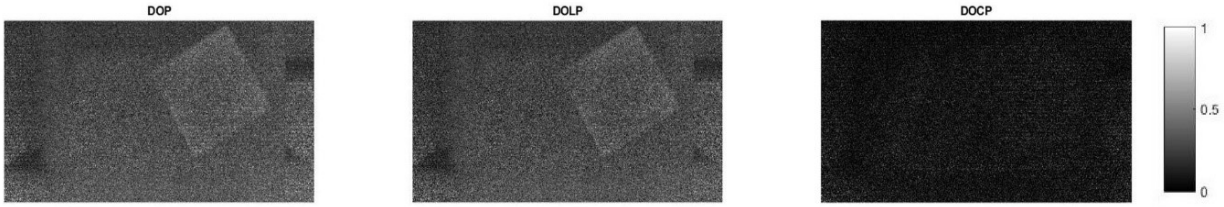

Figure 8. Maps of the recovered DOP, DOLP and DOCP for an image in reflection of a random linear state.

5. CONCLUSIONS

The system presented here constitutes a quite simple setup for an imaging imaging polarimeter together with its processing stages. Using very basic optical elements and a consumer CMOS, we have been able to build a polarimetric imaging device whose calibration results are very satisfying although some imperfections in the optical components may induce errors despite extending the improved calibration method for normal polarimeters to our system. Their maximum deviation error, lower than 10% in Stokes parameters estimation, validates the methodology used in order to calculate the measurement matrix **W** for a good calibration to perform polarimetric imaging. We believe these results can be improved if polarizers with higher extinction ratio are used.

ACKNOWLEDGMENTS

This work was supported by the Secretary of Universities and Research from the Generalitat of Catalunya and the European Social Fund under the grant 2018FI-B-00868 and partially supported by the Spanish Ministry of Economy and Competitiveness (MINECO) under the project FIS2017-89850R.

REFERENCES

[1] Tyo, J. S., Goldstein, D. L., Chenault, D. B., and Shaw, J. A., "Review of passive imaging polarimetry for remote sensing applications," *Appl. Opt.* **45**, 54535469 (2006).

[2] Snik, F., Craven-Jones, J., Escuti, M., Fineschi, S., Harrington, D., De Martino, A., Mawet, D., Riedi, J., and Tyo, J. S., "An overview of polarimetric sensing techniques and technology with applications to different research fields," *Proc. of SPIE* **9099**, 90990B (2014).

[3] Lewis, G., Jordan, D., and Roberts, P., "Backscattering target detection in a turbid medium by polarization discrimination," *Appl. Opt.* **38**, 39373944 (1999).

[4] Fade, J., Panigrahi, S., Carré, A., Frein, L., Hamel, C., Bretenaker, F., Ramachandran, H., and Alouini, M., "Long-range polarimetric imaging through fog," *Applied Optics* **53**(18), 3854 (2014).

[5] Sudarsanam, S., Mathew, J., Panigrahi, S., Fade, J., Alouini, M., and Ramachandran, H., "Real-time imaging through strongly scattering media: Seeing through turbid media, instantly," *Scientific Reports* **6**, 1–9 (2016).

[6] Deschamps, P. Y., Buriez, J. C., Bron, F. M., Leroy, M., Podaire, A., Bricaud, A., and Sze, G., "The polder mission: instrument characteristics and scientific objectives," *IEEE Trans. Geosci* **32**, 598–615 (1994).

[7] Novikova, T., Pierangelo, A., and Martino, A. D., "Polarimetric imaging for cancer diagnosis and staging," *Opt. Photonics News* **23**, 26–33 (2012).

[8] Pierangelo, A., Nazac, A., Benali, A., Validire, P., Cohen, H., Novikova, T., Ibrahim, B. H., Manhas, S., Fallet, C., Antonelli, M.-R., and Martino, A.-D., "Polarimetric imaging of uterine cervix: a case study," *Opt. Express* **21**, 1412014130 (2013).

[9] Trujillo-Bueno, J., Moreno-Insertis, F., Sanchez, F., DeglInnocenti, E. L., Stenflo, J. O., Mathys, G., Antonucci, R., Blandford, R., Agol, E., Broderick, A., Heyl, J., Koopmans, L., Lee, H.-W., Elitzur, M., Hildebrand, R. H., and Keller, C. U., [*Astrophysical Spectropolarimetry*], Cambridge University (2002).

[10] Boulbry, B., Ramella-Roman, J. C., and Germer, T. A., "Improved method for calibrating a Stokes polarimeter," *Appl. Opt.* **46**(35), 8533–8541 (2007).